Diamond & Related Materials 97 (2019) 107450

Contents lists available at ScienceDirect

Diamond & Related Materials

journal homepage: www.elsevier.com/locate/diamond

Tunable carrier density and high mobility of two-dimensional hole gases on diamond: The role of oxygen adsorption and surface roughness

D. Oing*, M. Geller, A. Lorke, N. Wöhrl

Department of Physics and CENIDE, University Duisburg-Essen, Lotharstr. 1, 47057 Duisburg, Germany

ARTICLE INFO

Keywords:
Two-dimensional hole gas
Single crystal diamond
Oxidation
P-type doping
Surface electronic properties

ABSTRACT

The transport properties of two-dimensional hole gases (2DHGs) on chemical-vapor-deposition (CVD)-grown diamond are investigated. A hydrogen plasma treatment and exposure to ambient atmosphere are used to establish and tailor the properties of the 2DHG. The transport parameters of the 2DHGs (namely carrier density and mobility) are characterized by temperature-dependent Hall measurements. The importance of the surface oxygen adsorption, determined by X-ray photoelectron spectroscopy (XPS), on the carrier density and mobility is shown. Hall measurements reveal that for oxygen concentrations below 2.2% (relative XPS signal) the carrier density is increasing from $1.4 \cdot 10^{10}$ cm^{-2} to $1.5 \cdot 10^{13}$ cm^{-2} with increasing oxygen adsorption. For oxygen concentrations above 2.2%, the charge carrier density decreases again. The carrier density remains constant over a temperature range between 4.2 K and 325 K. At room temperature, the mobility increases with decreasing carrier concentration. The opposite behavior is observed for 4.2 K.

By decreasing the surface roughness to 8.2 nm, we were able to increase the mobility to above 250 cm2/V s at room temperature for a carrier density of $1.2 \cdot 10^{13}$ cm^{-2}. This is among the highest values reported for 2DHGs on diamond.

1. Introduction

Diamond is a promising wide bandgap semiconductor with a bandgap of 5.5 eV, high charge carrier mobility of 3800 cm^2/V s for holes, 4500 cm^2/V s for electrons [1] and a high breakdown field of 10 MV/cm. However, diamond has a vanishing intrinsic charge carrier concentration, and all technologically relevant dopants have relative high activation energies (e.g. 360 meV for boron [2]). Therefore, the technically advantageous saturation regime is not reached.

A promising method to achieve saturation-like (temperature-independent) conductivity is based on the transfer doping mechanism [3], which leads to a two-dimensional hole gas (2DHG) on hydrogen-terminated diamond. Here, the lowest unoccupied energy level of adsorbates is below the valence band maximum of diamond. Therefore, electrons are transferred into these acceptor states and leave behind holes at the diamond surface, which form the 2DHG [3]. It was shown that ambient atmosphere can provide these acceptors. Possibly, H_3O^+-ions from a water layer are the responsible acceptors [3]. New results however, suggest that NO_2 [4,5] or rather NO_3^- [6] from the atmosphere induces the 2DHG.

In recent years, metal oxides attracted attention in literature. These metal oxides, e.g. Al_2O_3, possess the ability to substitute the already mentioned acceptor on the surface, while giving longtime and thermal stability [7]. Additionally, these metal oxides can be used as an insulator for field effect applications [8].

The transport properties of the 2DHG on diamond have been extensively studied and it was shown that they strongly depend on the surface properties (type of functionalization, crystallinity, roughness, crystal orientation). The carrier density reported in the literature ranges from $3.5 \cdot 10^{11}$ cm^{-2} [9] to $2.6 \cdot 10^{13}$ cm^{-2} [10] for samples exposed to ambient atmosphere. Samples exposed to NO_2-enriched atmosphere could reach carrier densities of up to $1.5 \cdot 10^{14}$ cm^{-2} on (110) surfaces [11]. Coated with transition metal oxides high carrier densities up to $2.5 \cdot 10^{14}$ cm^{-2} were achieved [12].

To explain these differences in carrier densities, Riedel et al. proposed that oxygen bound to the diamond surface is responsible for the electron transfer to the acceptor state at the surface [13]. Additionally, Wade et al. showed that the carrier density can be increased by increasing surface roughness [14] and explained the increase with the formation of “reactive sites”. Thus, three conditions must be fulfilled for a 2DHG to be formed: (i) hydrogen termination of the diamond surface, (ii) acceptor states at the surface and (iii) “reactive sites” that enables the electron transfer to said acceptors, although it is not completely clear what the “reactive sites” are [13,14].

* Corresponding author.
E-mail address: dennis.oing@uni-due.de (D. Oing).

https://doi.org/10.1016/j.diamond.2019.107450
Received 10 April 2019; Received in revised form 7 June 2019; Accepted 12 June 2019
Available online 13 June 2019
0925-9635/ © 2019 Elsevier B.V. All rights reserved.

The highest mobilities of 223 $cm^2/V\,s$ at room temperature for a carrier density of $6 \cdot 10^{11}$ cm^{-2} were observed on hydrogen-terminated diamond [15], which is much lower than the limit for undoped bulk diamond, having a mobility of 3800 $cm^2/V\,s$ [1]. The low mobility has been attributed to surface impurity scattering as the limiting factor and to surface roughness [16]. The surface impurity density is equal to the carrier density of the 2DHG and therefore the general trend in literature shows that the mobility decreases with increasing carrier density [9].

However, a complete understanding of the formation of the 2DHG and its transport properties, given by different parameters is still missing.

This work is intended to deepen the understanding of the influence of the amount of oxygen bound (C═O) to the surface on the transport properties of the 2DHG. For this purpose, the C═O concentration at the diamond surface was experimentally increased and quantitatively measured by XPS and the values correlated to the transport properties of the 2DHG over a wide temperature range (4.2 K up to room temperature). Additionally, a comparison of the transport properties of diamond samples with the same oxygen concentration but different surface roughness was made to investigate the influence of the roughness on the carrier mobility in more detail.

2. Experimental details

2.1. Sample fabrication

The substrates used were optical grade, single crystalline ⟨100⟩ oriented diamond chips (ElementSix) with sizes of 3 × 3 mm. A thin diamond film was synthesized using a custom-built Microwave Plasma-assisted CVD reactor based on a 2.45 GHz IPLAS *CYRANNUS* I-6″ plasma source [17]. The functional principle of this microwave plasma source is based on a resonator with annular slot antennas. This special setup allows for minimal interaction between the plasma and the reactor walls at the deposition pressure.

The samples were placed on a molybdenum substrate holder and the chamber was pumped down to $< 10^{-7}$ mbar. Prior to deposition, a hydrogen plasma was used to clean the sample and sample holder (200 mbar pressure, 2.6 kW microwave power, 400 sccm gas flow, 45 min exposure time). Two different deposition processes were used. The process parameters were 120 mbar, 1.26 kW, 500 sccm H_2, 57 sccm CH_4 for the first sample and 140 mbar, 1.5 kW, 376 sccm H_2, 24 sccm CH_4 for the second sample. The substrate temperature was 810 °C in both cases. The growth duration was 6 h and the growth rate was 6.5 μm/h for the first sample and 3.6 μm/h for the second sample. The samples were not polished to avoid the possible introduction of surface defects [18]. The resulting surface roughnesses were 8.2 nm and 21.1 nm for the first and second sample, respectively. Because of the missing polishing step, these surface roughnesses are higher than those in other studies.

Using a hydrogen generator (cmc Instruments GmbH type HG1200-2T) and a methane purifier (Mono Torr type PS4-MT3-531), a purity of the process gases of 7.0 (99.99999%) for hydrogen and 9.0 (99.9999999%) for CH_4 was achieved. The leakage of the vacuum chamber was estimated to be around $2.4 \cdot 10^{-4}$ sccm. This led to a nitrogen concentration of the grown layer below 1 ppb, based on an incorporation rate of 10^{-4} [19]. The nitrogen (n dopant) in the diamond films can also saturate the acceptor states at the surface and thus reduce the charge carrier density of the 2DHG. Taking the approach from Ristein et al. [20] we calculated that approximately $3.3 \cdot 10^{10}$ surface charges/cm^{-2} will not contribute to the 2DHG, but saturate the residual nitrogen doping. This is negligible compared to optical grade diamond films with a compensation charge density of approximately $1 \cdot 10^{12}$ cm^{-2}.

Metallic contacts to the 2DHG were fabricated by standard photolithography and evaporation of 10 nm NiCr as an adhesion layer and 100 nm Au. A Hall bar geometry was defined by selectively removing the 2DHG through an 18 s long oxygen plasma treatment, using photoresist as a protective mask. Fully oxygen terminated diamond is insulating [3]. We carefully measured the resistance in two point geometry to ensure that the plasma treatment lead to insulating surfaces. After processing, photoresist residues are found on the diamond surface, which could affect the transport properties as well as the X-ray photoelectron spectroscopy. Therefore, the remaining resist was removed using a hydrogen plasma treatment under conditions that etch the resist but do not affect the hydrogen or oxygen termination.

To increase the amount of oxygen on the surface and thus the concentration of the 2DHG, the sample was annealed at 200 °C under constant oxygen flow with a pressure of 8 mbar for various times as this is a durable method to increases the oxygen concentration on the diamond surface compared to UV treatments [21].

It has to be mentioned that there are several studies that show that the carrier density can change with small changes in the NO_2 concentration in the atmosphere [4,5,8] and in air-exposed samples due to small changes in temperature and humidity [7].

In this study, we have taken great care to avoid these negative influences by the environment. (i) Our samples were kept in ambient atmosphere for at least 1 day. This allowed the samples to reach an equilibrium state with the environment, as there were no changes in the conductivity after 3 h in ambient air were observed. Afterwards, the samples were mounted in a closed cryo-cycle cryostat with an inner vacuum chamber that was pumped down to a pressure of $< 10^{-5}$ mbar. The sample in the vacuum chamber establishes an extremely stable environment, hence, we could not see any changes in carrier density over the period of 3 days. All the XPS measurements were done under the same vacuum conditions.

2.2. Characterization

X-ray photoelectron spectroscopy (XPS) was used to determine the quantity of adsorbed oxygen. Aluminum K_α radiation was focused on a small area with a diameter of 50 μm. The charging of the surface was compensated using low energy electrons and Argon ions. The offset in binding energy was identified using an in situ sputtered copper foil.

The surface roughness was determined using an atomic force microscope at four different spots over an area of 25 × 25 μm^2.

The Hall voltage U_{xy} was measured in the closed cycle cryostat in magnetic fields $-2\ T \leq B \leq 2T$ with an increment of 0.05 T in the temperature range 4.2 K to 325 K. From the slope $\frac{dB}{dU_{xy}}$, the carrier density was calculated using $n = \frac{I_{SD}}{e}\frac{dB}{dU_{xy}}$, where I_{SD} is the current through the 2DHG. The conductance S was measured in 4-point geometry and the mobility was calculated as $\mu = \frac{a}{b} \bullet \frac{S}{en}$, where $\frac{a}{b}$ is the width-to-length ratio of the Hall bar.

3. Results and discussion

3.1. X-ray photoelectron spectroscopy (XPS)

Wide energy range XPS spectra are shown in Fig. 1a. For all spectra taken in this work, we could only observe a signal from the O 1s core-shell at a binding energy of 531.4 eV and the C 1s core-shell at 285 eV. To determine the amount of adsorbed oxygen, the C 1s (Fig. 1b) and O 1s (Fig. 1c) signals were deconvolved with a signal at 285.7 eV for the C 1s and 532.1 eV for the O 1s.

This signal is correlated to oxygen bounds to the diamond surface. By comparing these values with the literature this signal can be identified as C═O [22,23]. Taking the relative sensitivity factor *RSF* into account, the concentration was calculated from the area of the O 1s and the C 1s signal. The concentration shown in Fig. 1a is an average over both C═O signals. Additionally, the Auger signal (not shown here) from carbon was studied. The width of the Auger signal, the so-called D-parameter, is an indicator for the sp^2 to sp^3 ratio [24]. A width of 13 eV

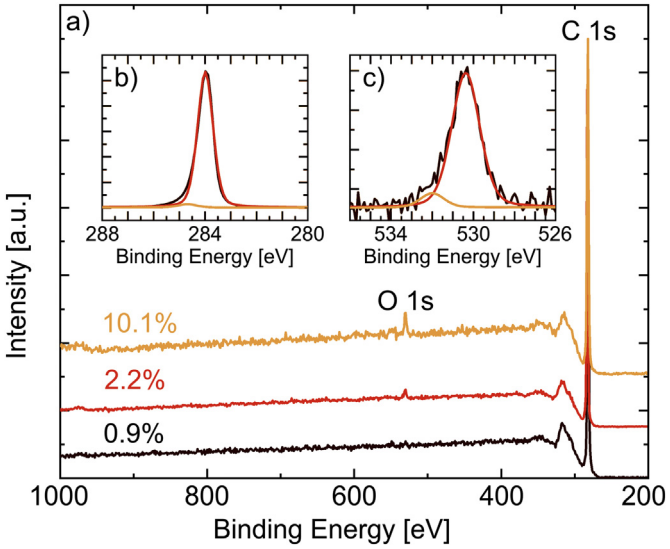

Fig. 1. XPS characterization of the synthesized diamond surfaces. a) Scan over a wide range of binding energies. Only signals for carbon and oxygen were observed. b) High resolution scan of the C 1s signal for an oxygen concentration of 2.2% with deconvolution for C═O (orange line). c) High resolution scan for O 1s signal for an oxygen concentration of 2.2% with C═O (orange line).

as measured for all samples in this work, shows that pure diamond without surface contamination (e.g. residual resist from processing) was observed in the Auger signal of the spectrum.

3.2. Charge carrier density

In the range between 0% and 0.6% oxygen adsorbed on the diamond surface, no conductivity of the 2DHG could be measured. For higher oxygen concentrations, the temperature-dependent hole carrier density is shown in Fig. 2b. Note that for some oxygen concentrations, data points are missing below a specific temperature. In these measurements, the mobility was less than 1 $cm^2/V\,s$ and we were unable to reliably determine the hole carrier density at low temperatures [26].

By increasing the oxygen adsorption from 0.7% to 1.7%, the hole carrier density increases by three orders of magnitude, i.e. from $1.1 \cdot 10^{10}$ cm^{-2} to $1.2 \cdot 10^{13}$ cm^{-2}. For oxygen adsorption above 1.7%, the increase is marginal to $1.5 \cdot 10^{13}$ cm^{-2}. This confirms the results from Riedel et al., who suspected that for low oxygen coverage the carrier density increases [13]. When increasing the oxygen adsorption to above 2.2%, the carrier density decreases and reaches $2.6 \cdot 10^{12}$ cm^{-2} for an oxygen concentration of 10.1%. The decrease of carrier density for higher oxygen coverage can be explained with the energetically unfavorable positive electron affinity of 1.7 eV for the C═O dipole, which increases the chemical potential of the acceptor with respect to the valence band maximum. This illustrates that oxygen fulfills two competing functions: (i) oxygen enables the electron transfer from the diamond surface to the acceptor states and (ii) oxygen is energetically unfavorable for the transfer compared to hydrogen. Fig. 2a shows that effect (i) is dominant for oxygen coverage below 2.2%, while effect (ii) is dominant for oxygen coverage above 2.2%.

Additionally, the carrier density is temperature independent down to 4.2 K. This is in contrast to results by Kubovic et al. [5], where a temperature dependence with an activation energy of 37 meV was observed.

To assess the influence of surface roughness on the hole carrier density, two sample were grown with roughness of 8.2 nm and 21.1 nm (root mean square, RMS). With 1.6% and 1.7%, respectively, the oxygen coverage of both samples was identical within the measurement accuracy. We found that for both samples, the measured carrier density is $1.2 \cdot 10^{13}$ cm^{-2}, which leads us to conclude that the "reactive sites" as mentioned in Ref [14] are related to adsorbed oxygen rather than edges and kinks caused by surface roughness. This is also in good agreement with the results from Crawford et al. who also measured similar carrier densities for different surface roughnesses [27]. The observation in [14] of an increasing carrier density with increasing surface roughness can be explained by increased oxygen adsorption at edges and kinks, where dangling bonds provide favorable binding sites for O atoms.

In Fig. 2a, the hole carrier density is shown for different oxygen coverage. To estimate the oxygen coverage, the density of surface carbon atoms is calculated by $(\textit{atomic density})^{2/3} \cdot [C = O]$. The density of adsorbed oxygen is for all measured values at least 4 times higher than the carrier density. Riedel et al. [13] suggested that each adsorbed oxygen creates one hole. In the range between 0.7% and 1.7% we can observe a one-to-one correspondence between oxygen coverage and hole carrier density. We also assume that this behavior is accurate for lower oxygen concentrations. However, the produced holes must first saturate charge traps on the surface.

As already mentioned in Section 2.1, the carrier density is

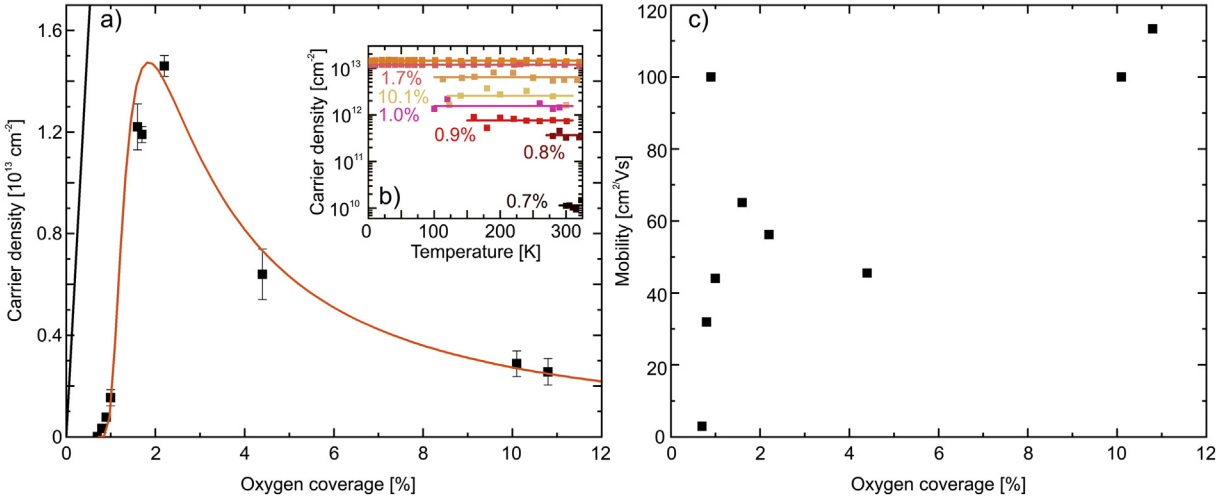

Fig. 2. a) Charge carrier density for different amounts of adsorbed oxygen. The black dots represent the measured charge carrier density. The black line illustrates the case when the charge carrier density of the 2DHG would correspond to C═O coverage. The orange line is a guide to the eye. b) Temperature dependent carrier density for different amounts of adsorbed oxygen. c) Mobility measured at room temperature for different oxygen coverage for the sample with rms = 21.1 nm. The corresponding carrier density can be seen in a).

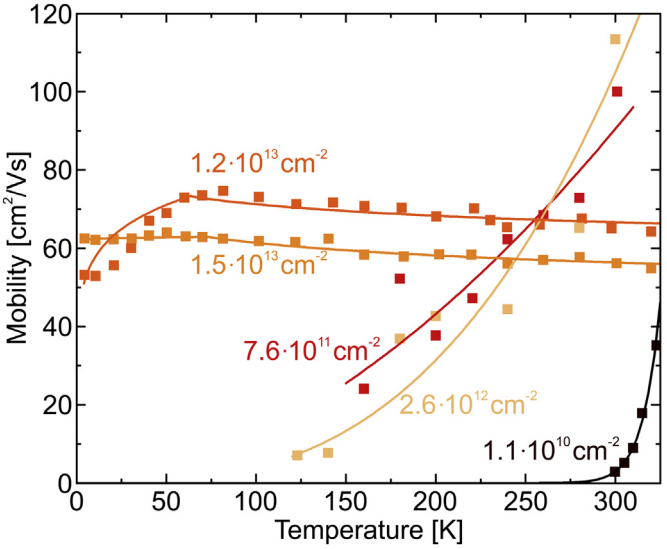

Fig. 3. Temperature dependent mobility for different amounts of adsorbed oxygen for a roughness of 21.1 nm. Lines are guides to the eye.

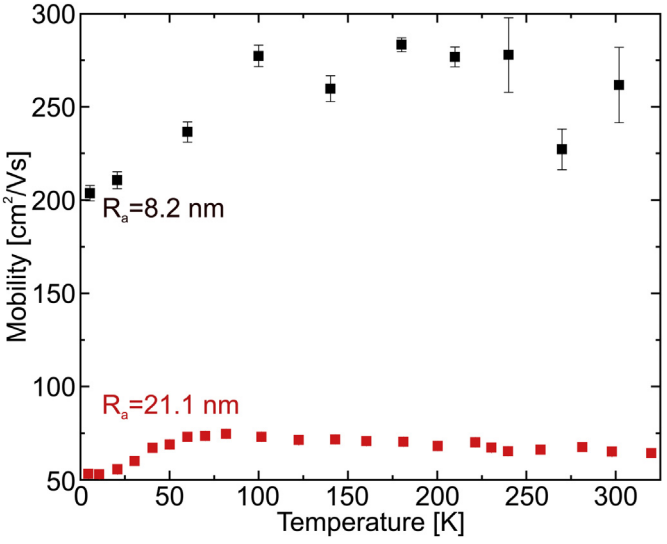

Fig. 4. Temperature dependent mobility of two different samples with the same carrier density and different roughness. The corresponding carrier densities are $1.19 \cdot 10^{13}$ cm^{-2} with a surface resistance of 8.1 kΩ at room temperature (red curve) and $1.22 \cdot 10^{13}$ cm^{-2} with a resistance of 2 kΩ at room temperature (black curve). (For interpretation of the references to color in this figure legend, the reader is referred to the web version of this article.)

dependent on the composition of ambient air [4,5,7,8]. We cannot exclude that the adsorbates formed on the diamond surface is the same after every annealing cycle. However, small changes in ambient air cannot explain an increase in carrier density by three orders of magnitude as the highest increase in carrier density due to strong changes in the environment is a factor of 7 [5]. Also, all measurements were performed under prolonged exposure to vacuum conditions.

3.3. Mobility

The temperature dependent mobility for different concentrations of adsorbed oxygen is shown in Fig. 3, corresponding to the measured hole carrier densities in Fig. 2.

For high carrier densities above $1 \cdot 10^{13}$ cm^{-2}, the mobility shows a weak temperature dependence between 4.2 K and 325 K. The low temperature dependence is attributed to screening effects of the 2DHG [25]. For carrier densities between $7 \cdot 10^{11}$ cm^{-2} and $1.5 \cdot 10^{13}$ cm^{-2} the mobility decreases with increasing carrier densities at room temperature but decreases strongly for lower temperatures. The high mobility at room temperature can be attributed to two possible reasons: (1) low surface impurity scattering due to the low density of acceptors at the surface [16], (2) decreasing surface roughness scattering with decreasing carrier density due to a weaker band bending and therefore higher separation of the carriers from the surface [25]. This explanation is further supported by the fact that the mobility at room temperature decreases with increasing carrier density. At lower temperature (e.g. $T \sim 160$ K) an increasing mobility can be observed with increasing carrier density. At low temperature, the ionized impurity scattering becomes more important, and a high carrier concentration more effectively screens the potential seen by 2DHG [16,25].

For carrier densities below $7 \cdot 10^{11}$ cm^{-2} the mobility is below $35 \frac{\text{cm}^2}{\text{V}}$s and decreases to < 1 cm^2/V s for temperatures below 280 K. This is attributed to weak screening for low carrier densities.

As already mentioned, for high carrier densities the surface roughness is an important effect. Therefore, the mobility can be increased by reducing the diamond surface roughness. This is demonstrated in Fig. 4, where the mobilities of the two samples 21.1 nm to 8.2 nm RMS roughness are compared. Both samples were prepared to have the same carrier density ($p = 1.2 \cdot 10^{13}$ cm^{-2}) to rule out the effects of surface impurity scattering and screening effects. It can be observed that the mobility increases from 65 cm^2/V s to 261.7 cm^2/V s at room temperature and from 55.6 cm^2/V s to 201.6 cm^2/V s at 20 K. Additionally, for low temperatures ($T < 60$ K) the mobility increases by increasing the temperature in both samples and then becomes weakly temperature dependent. We therefore suggest that both T-dependencies have the same origin and that the surface roughness scattering process is temperature independent, as already suggested by Li et al. [16].

4. Summary

Hydrogen-terminated diamond samples with low nitrogen bulk contamination were examined for their 2DHG transport properties at the surface. It was found that the concentration of adsorbed oxygen at the surface plays an important role. The dependence is non-monotonic and can be separated into two regions: (i) below an oxygen coverage of 2.2%, the carrier density increases by more than three order of magnitude, (ii) above 2.2%, the carrier density decreases again with oxygen coverage.

The coverage of oxygen at the surface was always higher than the carrier density. However, our data supports a model in which a one-to-one correspondence between oxygen coverage and hole carrier density exists, although only in a range between 0.7% and 1.7% oxygen coverage. It is also shown that the mobility is directly influenced by the carrier density. At room temperature, the mobility is limited by the high concentration of ionized adsorbates on the surface or by low screening dependent on the carrier density. At liquid helium temperature the mobility is limited by screening. The surface roughness scattering is a crucial factor at all temperatures. We observed a strong increase of the mobility to above 200 cm^2/V s when decreasing the roughness from above 20 nm to below 10 nm RMS.

Acknowledgements

We gratefully acknowledge support by Ulrich Hagemann from the Interdisciplinary Center for Analytics on the Nanoscale (ICAN).

References

[1] J. Isberg, J. Hammersberg, E. Johansson, T. Wikstro, D.J. Twitchen, A.J. Whitehead, S.E. Coe, G.A. Scarsbrook, High carrier mobility in single-crystal plasma-deposited diamond, Science 297 (2002) 1670, https://doi.org/10.1126/science.1074374.

[2] J. Achard, F. Silva, R. Issaoui, O. Brinza, A. Tallaire, H. Schneider, K. Isoird, H. Ding, S. Koné, M.A. Pinault, F. Jomard, A. Gicquel, Thick boron doped diamond single crystals for high power electronics, Diam. Relat. Mater. 20 (2011) 145–152, https://doi.org/10.1016/j.diamond.2010.11.014.
[3] F. Maier, M. Riedel, B. Mantel, J. Ristein, L. Ley, Origin of surface conductivity in diamond, Phys. Rev. Lett. 85 (2000) 3472, https://doi.org/10.1103/PhysRevLett.85.3472.
[4] M. Kubovic, M. Kasu, H. Kageshima, Sorption properties of NO2 gas and its strong influence on hole concentration of H-terminated diamond surfaces, Appl. Phys. Lett. 96 (2010) 052101, , https://doi.org/10.1063/1.3291616.
[5] M. Kubovic, M. Kasu, H. Kageshima, F. Maed, Electronic and surface properties of H-terminated diamond surface affected by NO_2 gas, Diam. Relat. Mater. 19 (2010) 889–893, https://doi.org/10.1016/j.diamond.2010.02.021.
[6] M.W. Geis, T.H. Fedynyshyn, M.E. Plaut, T.C. Wade, C.H. Wuorio, S.A. Vitale, J.O. Varghese, T.A. Grotjohn, R.J. Nemanich, M.A. Hollis, Chemical and semiconducting properties of NO_2-activated H-terminated diamond, Diam. Relat. Mater. 84 (2018) 86–94, https://doi.org/10.1016/j.diamond.2018.03.002.
[7] K.G. Crawford, D. Qi, J. McGlynn, T.G. Ivanov, P.B. Shah, J. Weil, A. Tallaire, A.Y. Ganin, D.A.J. Moran, Thermally stable, high performance transfer doping of diamond using transition metal oxides, Sci. Rep. 8 (2018) 3342, https://doi.org/10.1038/s41598-018-21579-4.
[8] M. Kasu, Diamond field-effect transistors for RF power electronics: novel NO_2 hole doping and low-temperature deposited Al_2O_3 passivation, Jpn. J. Appl. Phys. 56 (2017) 01AA01, https://doi.org/10.7567/JJAP.56.01AA01.
[9] C.E. Nebel, Surface transfer-doping of H-terminated diamond with adsorbates, New Diamond Front. Carbon Technol. 15 (2005) 247–264, https://doi.org/10.1063/1.3695643.
[10] N. Jiang, T. Ito, Electrical properties of surface conductive layers of homoepitaxial diamond films, J. Appl. Phys. 85 (1999) 8267–8273, https://doi.org/10.1063/1.370668.
[11] H. Sato, M. Kasu, Maximum hole concentration for hydrogen-terminated diamond surfaces with various surface orientations obtained by exposure to highly concentrated NO_2, Diam. Relat. Mater. 31 (2013) 47–49, https://doi.org/10.1016/j.diamond.2012.10.007.
[12] M. Tordjman, K. Weinfeld, R. Kalish, Boosting surface charge-transfer doping efficiency and robustness of diamond with WO3 and ReO_3, Appl. Phys. Lett. 111 (2017) 111601, , https://doi.org/10.1063/1.4986339.
[13] M. Riedel, J. Ristein, L. Ley, Recovery of surface conductivity of H-terminated diamond after thermal annealing in vacuum, Phys. Rev. B 69 (2004) 125338, , https://doi.org/10.1103/PhysRevB.69.125338.
[14] T. Wade, M.W. Geis, T.H. Fedynyshyn, S.A. Vitale, J.O. Varghese, D.M. Lennon, T.A. Grotjohn, R.J. Nemanich, M.A. Hollis, Effect of surface roughness and H–termination chemistry on diamond's semiconducting surface conductance, Diam. Relat. Mater. 76 (2017) 79–85, https://doi.org/10.1016/j.diamond.2017.04.012.
[15] B. Rezek, H. Watanabe, C.E. Nebel, High carrier mobility on hydrogen terminated < 100 > diamond surfaces, J. Appl. Phys. 88 (2006) 042110, https://doi.org/10.1063/1.2168497.
[16] Y. Li, J. Zhang, G. Liu, Z. Ren, J. Zhang, Y. Hao, Mobility of two-dimensional hole gas in H-terminated diamond, Phys. Status Solidi Rapid Res. Lett. 12 (2018) 1700401, https://doi.org/10.1002/pssr.201700401.
[17] CYRANNUS I, European Patent No. 0 872 164, USA Patent No. 6,198,224.
[18] J. Achard, F. Silva, O. Brinza, X. Bonnin, V. Mille, R. Issaoui, M. Kasu, A. Gicquel, Identification of etch-pit crystallographic faces induced on diamond surface by H2/O2 etching plasma treatment, Phys. Status Solidi A 206 (2009) 1949–1954, https://doi.org/10.1002/pssa.200982210.
[19] S. Jin, T.D. Moustakas, Effect of nitrogen on the growth of diamond films, Appl. Phys. Lett. 65 (1994) 403, https://doi.org/10.1063/1.112315.
[20] J. Ristein, M. Riedel, F. Maier, B.F. Mantel, M. Stammler, L. Ley, Surface conductivity of diamond as a function of nitrogen doping, Phys. Status Solidi (a) 186 (2001) 249–256, https://doi.org/10.1002/1521-396X(200108)186:2<249::AID-PSSA249>3.0.CO;2-6.
[21] S. Torrengo, L. Minati, M. Filippi, A. Miotello, M. Ferrari, A. Chiasera, E. Vittone, A. Pasquarelli, M. Dipalo, E. Kohn, G. Speranza, XPS and UPS investigation of the diamond surface oxidation by UV irradiation, Diam. Relat. Mater. 18 (2009) 5–8, https://doi.org/10.1016/j.diamond.2009.02.003.
[22] J. F. Moulder, W. F. Stickle, P. E. Sobol, K. D. Bomben, Handbook of X-ray Photoelectron Spectroscopy, Physical Electronics, Inc. (1995).
[23] G.P. Lopez, D.G. Castner, B.D. Ratner, XPS O1s binding energies for polymers containing hydroxyl, ether, ketone and ester groups, Surf. Interface Anal. 17 (1991) 267–272, https://doi.org/10.1002/sia.740170508.
[24] S. Turgeon, R.W. Paynter, On the determination of carbon sp2/sp3 ratios in polystyrene–polyethylene copolymers by photoelectron spectroscopy, Thin Solid Films 394 (2001) 44–48, https://doi.org/10.1016/s0040-6090(01)01134-8.
[25] T. Ando, Electronic properties of two-dimensional systems, Rev. Mod. Phys. 54 (2) (1982), https://doi.org/10.1103/RevModPhys.54.437.
[26] A. Gondorf, M. Geller, J. Weißbon, A. Lorke, Mobility and carrier density in nanoporous indium tin oxide films, Phys. Rev. B 83 (2011) 212201, , https://doi.org/10.1103/physrevb.83.212201.
[27] K.G. Crawford, A. Tallaire, X. Li, D.A. Macdonald, D. Qi, D.A.J. Moran, The role of hydrogen plasma power on surface roughness and carrier transport in transfer-doped H-diamond, Diam. Relat. Mater. 84 (2018) 48–54, https://doi.org/10.1016/j.diamond.2018.03.005.